

Highly sensitive detection of cephadrine based on three-dimensional honeycomb-like porous nano-silver

S. Li ^a, Y. Zhang ^a, S. Sun ^a, L. Zeng ^a, F. He ^{a,b,*}

^a College of Pharmacy, Shaoyang University, Shaoyang 422000, China

^b Key Laboratory of Chemical Biology and Traditional Chinese Medicine Research (Ministry of Education), College of Chemistry and Chemical Engineering, Hunan Normal University, Changsha 410081, China

In this paper, three-dimensional honeycomb-like porous nano-silver (3DHPNS) were prepared by one-step potentiostatic deposition on bare gold electrode by using dynamic bubble template method. The electrochemical behavior of 3DHPNS modified Au (3DHPNS/Au) electrode in 0.1 M phosphoric acid buffer solution (pH=7.0) was studied, and the electrocatalytic properties and sensing properties of cephadrine (CEP) on the 3DHPNS/Au electrode were investigated. Due to the large specific surface area and high porosity of 3DHPNS, which can supply more catalytic active sites and accelerate the mass transfer rate, the 3DHPNS/Au electrode show superior electrocatalytic activity and sensing performance of CEP.

(Received January 6, 2025; Accepted May 10, 2025)

Keywords: Three-dimensional honeycomb-like porous nano-silver, Cephadrine, Dynamic bubble template method, Electrocatalytic activity

1. Introduction

Metal nanomaterials with unique magnetic, electrical, optical and thermal properties are widely used in optoelectronic devices, physical structures, chemical catalysis, biosensing, agriculture and medical related fields[1]. Secondly, metal nanomaterials have mesoscopic properties, such as mechanical properties, thermal properties, optical properties and dielectric limiting effect, which are different from common materials and atoms or molecules[2, 3]. And their small size, but large specific surface area, and many uncoordinated atoms exist on the surface atoms result in enhanced activity of surface atoms and high catalytic activity[4-6]. In order to expand the application prospects and fields of metal nanomaterials, more and more people begin to study and innovate new structures of metal nanomaterials[7]. Compared with the two-dimensional planar structure and other three-dimensional structures, the three-dimensional honeycomb porous nanostructure enables the metal nanomaterials to have uniform nanochannels, smaller size and large specific surface area, which can better exert their superior sensitivity, electrochemical stability, adsorption, low preparation cost and wider application range[8, 9]. Therefore, in the past

* Corresponding author: hefang20101227@163.com

<https://doi.org/10.15251/DJNB.2025.202.493>

decade, nanomaterials with this structure have become a research hotspot. Among many different three-dimensional porous nano-metal materials, silver has the advantages of suitable price, easy preparation[10], stable performance[11], will not cause environmental pollution[12], and is not easily corroded[13], had a good reusability[14] and so on[15]. So, the application value of three-dimensional honeycomb nano-silver is worth further development.

The structure and morphology of metal nanomaterials are important factors affecting their properties. The results show that the dynamic bubble template electrodeposition method has the highlights of low cost, simple operation, high controllability and convenient preparation by one-step electrodeposition[16-20]. As early as many years ago, some scholars have prepared a variety of copper films with different structure using hydrogen bubbles as the dynamic template[21, 22]. The copper film has significant super-hydrophobicity and can be used in biomedicine and other fields. Subsequently, some scholars used the same method to prepare porous gold films, and the obtained gold films showed excellent catalytic activity for the electrooxidation of glucose[23]. Yang et al. also used deposition method to prepare three-dimensional porous polypyrrole-derived graphene electrode, showing superior catalytic performance and advanced electrode properties, which is expected to be used in catalytic field[16]. Because the dynamic bubble template method is simple to prepare, many scientists have applied this method to prepare a variety of different metal porous nanomaterials for many fields[24]. Therefore, dynamic bubble template method to prepare three-dimensional porous metal nano-materials has attracted tremendous attentions in recent decades. However, there are few reports about the application of three-dimensional honeycomb porous metal nanomaterial modified electrode for antibiotic drug detection.

Cephadrine (CEP), the first generation of cephalosporin antibiotics, has obvious antibacterial effect on drug-resistant bacteria, which is cheap and widely used[25]. Nowadays, the society develops rapidly and the level of science and technology advances by leaps and bounds. Medicine has become a special commodity in human daily life, and drug safety is also directly affect people's health and life safety[26]. The current drug safety problems are emerging in an endless stream, especially the abuse of antibiotics has become a key concern of the society. Antibiotic resistance is one of our most serious global health threats[27, 28], because it make challenging to fight many easily treatable diseases and will end up eliminating antibiotic clinical value over time[29, 30]. Therefore, it is of important significance to develop an effective, rapid and sensitive sensor for CEP detection[31, 32].

Electrochemical sensor is a kind of sensor that uses electrochemical principles to detect chemical substances, which realizes quantitative analysis by measuring the current or potential change generated by the reaction of electrodes with chemical substances[33]. In the antibiotic detecting field, electrochemical sensors have attracted wide attention because of their bright spots of great sensitivity, fast response, simple operation and highly cost effective[34-37]. During the detection process, antibiotic molecules interact specifically with certain functional groups on the surface of the working electrode or with immobilized biometric elements[38, 39]. These interactions cause a change in the charge distribution on the electrode surface, resulting in a change in current or potential. By measuring these changes, the concentration of antibiotics in the sample can be quantitatively analyzed[40]. Therefore, in the detection process, the catalytic activity of the electrode material used and the detection environment have an important impact on the detection results[41].

In view of this, the three-dimensional honeycomb-like porous nano-silver(3DHPNS) were prepared on bare gold electrodes by dynamic bubble template method, for the detection of the antibiotic CEP. The 3DHPNS was prepared by controlling electrodeposition potential, deposition time, electrolyte concentration and other factors. The electrocatalytic activity of 3DHPNS/Au modified electrode on CEP under neutral pH were investigated. Under optimal conditions, the 3DHPNS/Au electrode has good CEP sensing performance, the linear range is $2.5 \times 10^{-2} \text{ mM} \sim 1.13 \text{ mM}$, the detection limit is $1.0 \times 10^{-7} \text{ M}$, and the sensitivity is $326 \mu\text{A mM}^{-1} \text{ cm}^{-2}$. The application of this kind of electrode to the detection of antibiotics to improve the detection performance has certain guiding and practical significance for the detection of antibiotics.

2. Experimental materials and methods

2.1. Instrumentation and chemicals

All electrochemical experiments were performed on a CHI660E electrochemical workstation (Shanghai ChenHua Instruments Co., China) and a conventional three-electrode electrolytic cell was used. SEM (JEM-6700F field emission scanning electron microscope) were applied to characterize the structure of composites.

Silver nitrate and ammonia were purchased from Shanghai Reagent Company, ammonium chloride was purchased from Tianjin Kemiou Reagent Company, anhydrous ethanol and sodium hydroxide were purchased from Beijing Chemical Reagent Co., LTD., and CEP was purchased from Hayao Group. All chemical reagents were analytically pure or higher, and it can be purchased on the market. The solution was prepared in Millipore ultra-pure water ($\geq 18 \text{ M}\Omega \text{ cm}$). All experiments were carried out at room temperature of about 25°C .

2.2. Cleaning and characterization of bare gold electrode

The electrode surface was polished with fine sandpaper for preliminary cleaning, and then polished with alumina polishing powder. After that, physical ultrasonic cleaning was carried out in water—95% anhydrous ethanol solution—water for 5 minutes. Followed by chemical cleaning, a mixture of $\text{V}(\text{H}_2\text{SO}_4) : \text{V}(\text{H}_2\text{O}_2) 3:1$ was added to the surface of the bare gold electrode, and cleaned 2-3 times for 3 minutes each time[42]; The next step is electrochemical cleaning. The three electrodes (bare gold electrode, glassy carbon electrode and calomel electrode) are connected to the electrochemical workstation and placed in 0.5M concentrated sulfuric acid. First, high potential (scanning voltage is 2V) is cleaned, then low potential (scanning voltage is -0.35V) is cleaned, and finally cyclic voltammetry (-0.35V \sim 1.55V) is cleaned and characterized [43].

The three electrodes were placed in a mixed solution of 0.1M Na_2SO_4 and 2mM $\text{K}_4[\text{Fe}(\text{CN})_6]$, and the cyclic voltammetry was performed using the CHI 660E electrochemical workstation (scanning voltage was -0.1 \sim -0.5V, scanning speed was 100 mV/s). The appearance of a pair of regular shape REDOX peaks (peak potential width of about 80 mV), indicating that potassium ferricyanide is easy to reach the electrode surface REDOX reaction, the electrode surface has been cleaned [44-46].

2.3. Preparation of 3DHPNS modified electrode

The cleaned bare gold electrode was placed in a solution (total volume: 20 mL) composed of 0.01 M AgNO_3 , 1.0 M $\text{NH}_3 \cdot \text{H}_2\text{O}$ and 1.5 M NH_4Cl , and a constant voltage of -4 V was applied to prepare the 3DHPNS/Au electrode by dynamic bubble template method[47, 48], at the same time, Ag^+ electrodeposited between the bubbles and attached to the surface of the bare gold electrode. In the electrodeposition process, we can see that the bubbles on the electrode surface are formed, merged and enlarged, and precipitated rapidly, while the metal electrodeposition also occurs. Since there are more electrolytes between the bubbles and more electrode surface active sites, it can be inferred that metal deposition occurs in the gaps between the bubbles. After washing simply, the modified electrode was utilized to following electrochemical studies.

3. Results and discussion

3.1. Characterization of 3DHPNS/Au modified electrode

We use the SE detector to zoom in and see that the surface of the electrode with honeycomb-like porous structure is shown in Figure 1. It can be confirmed that the 3DHPNS/Au modified electrode has been prepared. Compared with the bare gold electrode and the nano-silver modified electrode prepared by conventional electrodeposition, the prepared electrode has larger specific surface area, porosity and catalytic active site.

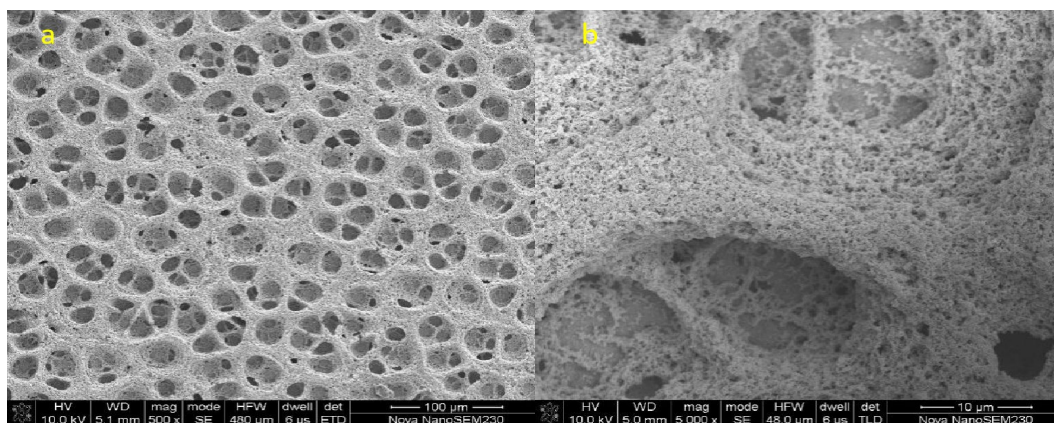


Fig. 1. (a) The 3DHPNS/Au electrode surface was observed at a high voltage of 10kv at a working distance of 5.1 mm using an SE detector amplified 500 times; (b) The 3DHPNS/Au electrode surface was observed at a high voltage of 10kv at a working distance of 8.2 mm using an SE detector amplified by 5000 times.

The cyclic voltammetry characterization of the prepared 3DHPNS/Au modified electrode (in a mixture of 0.1M Na_2SO_4 and 2 mM $\text{K}_4[\text{Fe}(\text{CN})_6]$) was similar to that of the bare gold electrode, and a pair of regularized REDOX peaks appeared, and the REDOX peak potential was wide, similar to that of the bare electrode, and not higher than 80mV. The results show that the 3DHPNS/Au electrode with three-dimensional honeycomb porous structure prepared by us has excellent conductivity, even better than that of bare electrode.

3.2. Electrocatalytic performance of different silver-plated electrode for CEP

We studied the comparison of detection efficiency between bare gold electrode, ordinary nano silver electrode and three-dimensional honeycomb nano silver electrode. Figure 2 shows that the DPV response at the bare gold electrode, ammonium chloride silver-plated electrode, sodium chloride silver-plated electrode and the hydrochloric acid silver-plated electrode recorded from -1.0 V to -0.4 V in PBS buffer (pH=7.0) containing 0.75 mM CEP. There is the lowest DPV response of the bare gold electrode, and there are no obviously distinctions of the hydrochloric acid silver-plated electrode and sodium chloride silver-plated electrode while a prominent enhanced signal was obtained on the hydrochloric acid silver plated electrode. In contrast, the ammonium chloride silver plated electrode has a significant enhanced signal than the other three electrodes, emphasizing the importance of the ammonium chloride in silver plating process. We have proved that the silver-plated electrode prepared in ammonium chloride solution has better electrical conductivity and a larger specific surface area. Therefore, this method will be used to prepare the 3DHPNS/Au electrode for the determination of CEP.

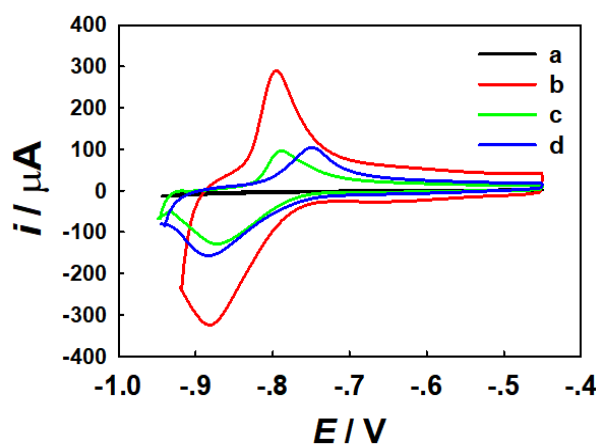


Fig. 2. The current response values of bare gold electrode (a), the ammonium chloride silver-plated electrode (b), the sodium chloride silver-plated electrode (c), and the hydrochloric acid silver-plated electrode (d). Current i is the current response value of the three electrodes to CEP after adding 0.75mM CEP to PBS buffer.

3.3. Electrocatalytic performance of 3DHPNS/Au electrode for CEP

We tested the current response of the 3DHPNS/Au electrode at different scan rates (0.1, 0.3, 0.5, 0.9, 1.5 V s⁻¹). The result show that the current response increases multiply with the increase of the scanning rate. The current response is lowest when the scan rate is 0.1V/s, and increases to 1800 μ A when the scan rate is increased to 1.5 V/s. So, the peak current value has a great linear relationship with the scanning rate. From this, we infer that the electrode reaction is controlled by adsorption (as shown in Figure 3), and the CEP electrode reaction process is an irreversible process controlled by adsorption [22]. In the determination process, the higher the scanning rate, the larger the peak current.

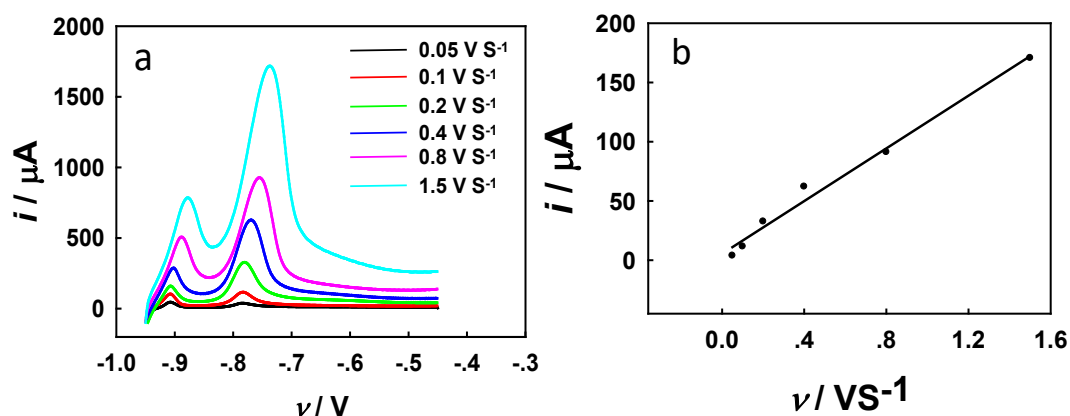


Fig. 3. Current response of 3DHPNS/Au electrode to CEP at different scan rate. (a) The current i is the continuous current response of the 3DHPNS/Au electrode to the CEP after adding 0.75mM CEP to the PBS buffer; (b) The relationship of scan rate with the peak current value of 3DHPNS/Au electrode to CEP after adding 0.75mM CEP to the PBS.

3.4. Optimization of the plating conditions

In the process of electroplating preparation of three-dimensional honeycomb silver, electroplating conditions affect the structure and micro-morphology of 3DHPNS, and thus affect the detection effect of CEP. To get better sensitivity of the 3DHPNS/Au modified electrode for CEP, a few significant parameters were researched as follow. Firstly, the concentration of NH_4Cl solution used to prepare 3DHPNS/Au electrode was optimized. Figure 4a shows that the current response value of 3DHPNS/Au electrode to CEP changes with the change of NH_4Cl concentration. When the concentration of ammonium chloride is in the range of 0.5 M to 1.5 M, the current response value increases with the increase of concentration. However, when the concentration of NH_4Cl solution is higher than 1.5 M, the current response value decreases with the increase of the concentration. Thus, 1.5 M NH_4Cl solution can achieve the highest sensitivity of detection. It is speculated that NH_4Cl solution in electroplating solution affects the speed of gas evolution during electrodeposition. The higher the concentration of NH_4Cl , the more bubble sources, the faster the gas evolution speed, resulting in higher porosity of 3DHPNS deposited. However, the concentration of NH_4Cl is too large and the gas evolution is too fast, which will hinder the metal electrodeposition and reduce the quality of the electrode surface electroplating, which is not conducive to the formation of 3DHPNS. Therefore, concentration 1.5 M of NH_4Cl solution was used for the following experiment.

The influence of $\text{NH}_3\cdot\text{H}_2\text{O}$ solution concentration was studied within the scope of 0.5 M to 1.5 M in quick succession, as shown in Figure 4b. The current response value of 3DHPNS/Au electrode increase with increasing the $\text{NH}_3\cdot\text{H}_2\text{O}$ concentration from 0.5 M to 1.0 M and then attain the highest response at 1.0 M, but lower response is revealed from 1.0 M to 1.5 M nevertheless. The reason may be the addition of $\text{NH}_3\cdot\text{H}_2\text{O}$ in the solution can form a complex with Ag^+ , and then prevent Ag^+ ions from combining with Cl^- in the solution to generate AgCl precipitation and reduce the content of Ag^+ in the solution. But adding too much $\text{NH}_3\cdot\text{H}_2\text{O}$ to the electroplating solution will cause the pH of the solution to increase, which is not conducive to the electrolysis of NH_4^+ to produce hydrogen bubbles. Thus, the $\text{NH}_3\cdot\text{H}_2\text{O}$ concentration of 1.0 M was the optimal concentration selected for the subsequent study.

It is thus interesting to compare the current of the different deposition times and potential in the 1.5 M NH_4Cl and 1.0 M $\text{NH}_3\cdot\text{H}_2\text{O}$ solution, as shown in Figure 4c and Figure 4d. Not hard to see that the currents for electrode rise with the deposition potential decreasing from -2.0 to -5.0 V, and yet the currents decreased after the potential less than -5.0 V. The electrochemical response of the electrode improved with the increase of the deposition time from 50 s to 150 s. But, with the extension of the deposition time, the current not only did not increase, but also decreased a lot. As a result, the best deposition potential and time was -5.0 V and 150 s, severally.

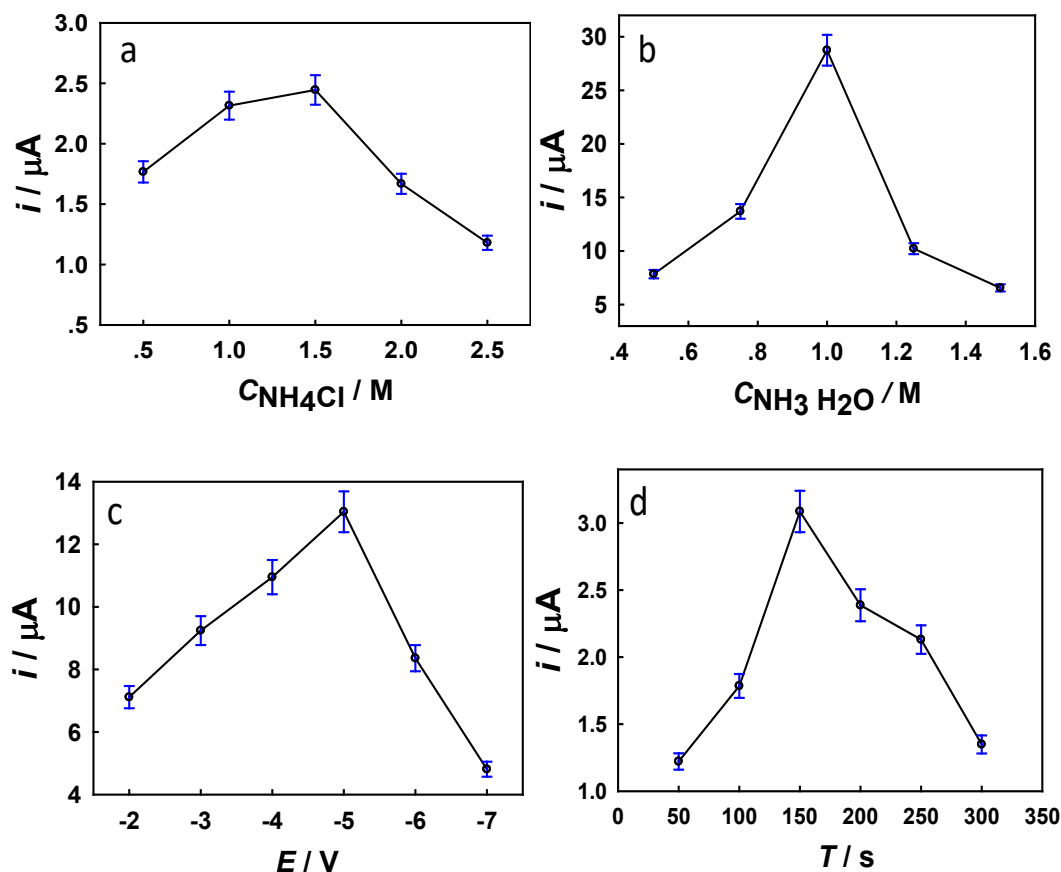


Fig. 4. Optimization diagram of (a) ammonium chloride concentration, (b) ammonia concentration, (c) electrodeposition time and (d) electrodeposition potential in electrodeposition solution of 3DHPNS/Au, the current i is the peak current value of the 3DHPNS/Au electrode to the CEP after adding 0.75mM CEP to the PBS buffer (The detection potential is 100mV).

3.5. Optimization of the detection conditions

In the process of CEP detection, the condition of the detection solution plays a crucial role in the detection effect and sensing performance. During the experiment, we set up the detection environment with five different pH values, and other conditions related to the detection were completely consistent. The test solutions were all PBS buffer solutions, and the pH of the test environment was adjusted by adding standard HCl solution and standard NaOH solution[49]. Figure 5 shows that pH 7 of PBS buffer solution, the 3DHPNS/Au electrode has the highest

response value to CEP. Therefore, we chose a PBS buffer solution with pH 7.0 as the supporting electrolyte.

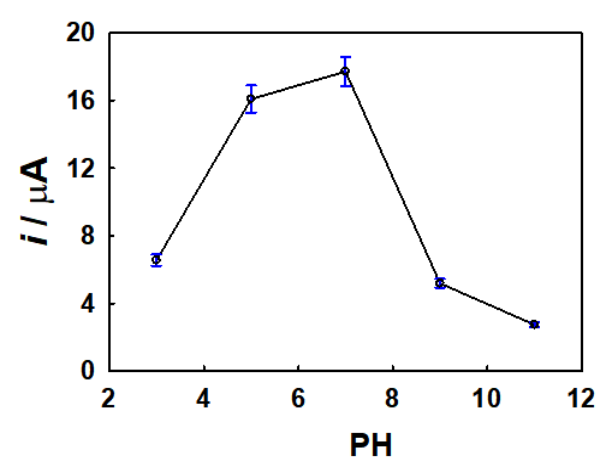


Fig. 5. Optimization diagram of the pH values in the test solution, the current i is the peak current value of the 3DHPNS/Au electrode to the CEP after adding 0.75mM CEP to the PBS buffer.

3.6. The establishment of working curve

After preparing a series of CEP solutions with gradient concentrations ($2.5 \times 10^{-2} \text{ M} \sim 1.75 \text{ M}$), the electrochemical differential pulse voltammetry (DPV) was used to detect CEP, and the detection curve of the response of 3DHPNS/Au electrodes to different concentrations of CEP was recorded, as shown in Figure 6a. The experimental results show that with the gradual increase of CEP concentration, the oxidation peak current also increases gradually, the current response value also increases. Within a certain range, the CEP concentration has a linear relationship with the current value of the oxidation peak (as shown in Figure 6b). The 3DHPNS/Au electrode is sensitive to CEP, with a linear range of $2.5 \times 10^{-2} \text{ mM} \sim 1.13 \text{ mM}$ and a sensitivity of $326 \mu\text{A mM}^{-1} \text{ cm}^{-2}$. Compared with other reports, the sensor we prepared has obvious advantages, such as wide linear range and high sensitivity. Combined with the electrocatalytic activity of silver metal on CEP, the 3DHPNS electrode prepared by us shows better sensing performance, and the high porosity of 3DHPNS can accelerate the mass transfer rate and further improve the sensor performance.

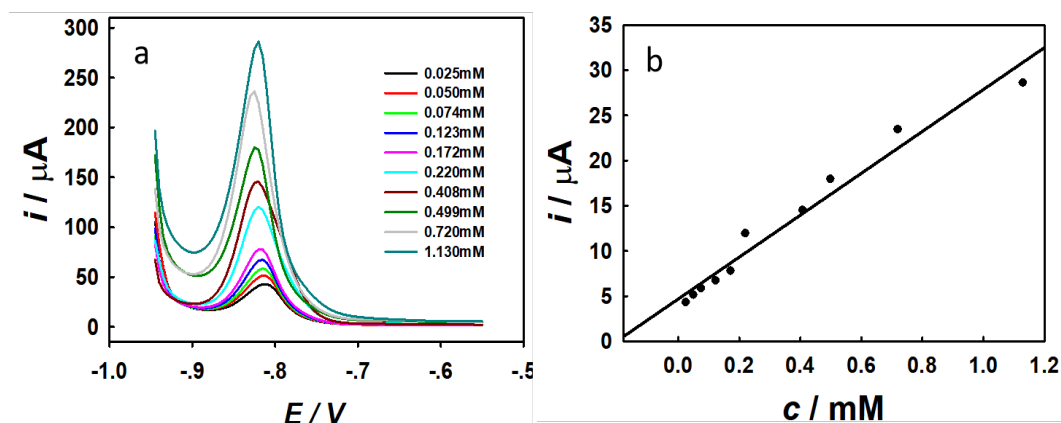


Fig. 6. (a) DPV response diagram of 3DHPNS/Au electrode to different concentrations of CEP solution (detection solution: PBS buffer, potential width: 0.01s, sweep speed: 0.07V). (b) Relationship between different concentration of CEP solution and the peak current value.

Table 1. Some modified electrode sensing performance.

Fabrication	The measuring object	Sensitivity / $\mu\text{AmM}^{-1}\text{cm}^2$	LOD / μM	LDR / μM	Method	Reference
BDD	MTZ	-	0.065	0.020-4.2	SWV	[50]
Nano-SrWO ₄	SDZ	0.123	0.009	0.009-235.0	CV	[51]
Apt-UCNPs	DOX	-	0.50	0.50-55.0	Fluorescence	[52]
3DHPNG/Au	Glucose	316	0.22	0.02-17.3	CV	[43]
EGr/GC	AZT	680	0.003	0.0003-10.0	DPV	[53]
SPE/rGO-NHS-AuNFs	CAP	-	0.001	0.001-10.0	CV	[54]
3DHPNS/Au	CEP	326	0.1	0.025-1.13	DPV	This work
AgNPs/SF-GR/GCE	CAP	-	0.01	0.01-20.0	DPV	[55]
	MTZ	-	0.05	0.05-20.0		

MTZ: metronidazole; SDZ: sulfadiazine; DOX: doxorubicin; AZT: azithromycin; CAP: chloramphenicol; SWV: square wave voltammetry; CV: cyclic voltammetry; DPV: differential pulse voltammetry.

3.7. Experimental stability and anti-interference

We evaluated the operational stability, storage stability and anti-interference of the prepared CEP sensors. The relative standard deviation (RSD) of the current response for 5 consecutive measurements of the same concentration of CEP was 4.9% ($n = 5$), indicating good operational stability of the biosensor (Figure 7a). In addition, after the CEP was prepared into a standard solution of a certain concentration, it was heated on a magnetic stirrer at 100°C for 20 minutes to degrade the CEP drug, and then cooled to room temperature for use. In order to investigate its storage stability, CEP was detected every two hours in this experiment. The experimental results show that the storage stability decreases with the passing of time within 10 hours, but the decreasing trend is moderate, and the overall stability is good (as shown in Figure 7b).

Under the optimal test conditions, the oxidation peak current of the drug to be tested before and after the addition of the interferant was compared. The experiment results expressed that the REDOX peak current of CEP was not affected even when other cephalosporins (ceftriaxone, ceftazidime) with the same concentration were present, so other cephalosporins had no obvious interference. And tests revealed that when the concentration of L- (+) -ascorbic acid is 3 times that of CEP, the REDOX peak current decreases obviously, so the higher concentrations of L- (+) -ascorbic acid presented significant interference. However, when Na^+ with a concentration 1500 times that of CEP was added to the solution, the REDOX peak current was slightly reduced, so Na^+ interfered slightly with the detection of CEP (Figure 7c). Therefore, when carrying out complex sample determination, it is necessary to adopt certain pre-treatment methods to separate the substances that cause interference.

Table 2. Different serial numbers represent the interfering substance and its concentration ratio.

Serial number	Added substance	$C_{\text{Others}}/C_{\text{CEP}}$
1	CEP	-
2	CEP + ceftazidime	1
3	CEP + ceftriaxone	1
4	ceftazidime	-
5	ceftriaxone	-
6	CEP + L- (+) -ascorbic acid	3
7	CEP + Na^+	1500

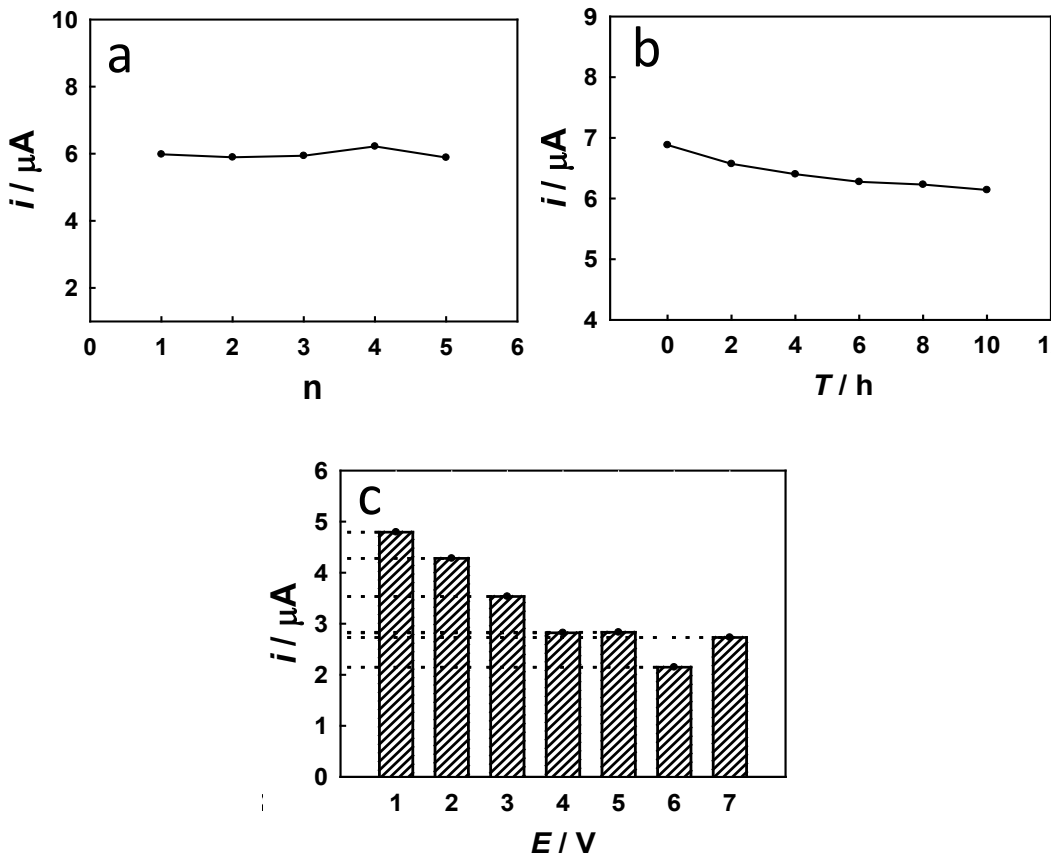


Fig. 7. (a) The current response value of the 3DHPNS/Au electrode to the CEP for 5 consecutive times during storage. (b) The current response value of the 3DHPNS/Au electrode to the CEP for 6 consecutive times every 2 hours during storage. (c) The current response value of the 3DHPNS/Au electrode to the detected substance after adding different substances. (The detection potential is 100mV).

4. Conclusions

In summary, a three-dimensional honeycomb porous nanosilver (3DHPNS) modified electrode was made by dynamic bubble template method, and its porous structure was used to improve the detection effect of the modified electrode[56, 57]. In order to make the detection results more sensitive, the preparation conditions of 3DHPNS modified electrode, detection conditions, storage stability, operation stability and experimental anti-interference of CEP sensor were studied in detail.

The results indicated that with the preparation conditions, the 3DHPNS modified electrode prepared by electroplating had the best performance for CEP detection at 1.5 M NH_4Cl concentration, 1.0 M $\text{NH}_3 \cdot \text{H}_2\text{O}$ concentration, 150 s deposition time and -5 V deposition potential. When 0.1M PBS buffer solution with pH=7.0 was used as pH detection condition, the response value was the highest. The 3DHPNS/Au electrode has good sensing performance for CEP. The linear detection range is $2.5 \times 10^{-2} \text{ mM} \sim 1.13 \text{ mM}$, the detection limit is $1.0 \times 10^{-7} \text{ M}$, and the sensitivity is $326 \mu\text{A mM}^{-1} \text{ cm}^{-2}$. In addition, the storage stability, operation stability and experimental anti-interference performance of the CEP sensor are good.

At present, nano-silver has been widely used in clinical drug detection and plays an important role, but the application of nano-silver with three-dimensional honeycomb structure is very few. The three-dimensional honeycomb structure has a large specific surface area, as well as good porosity and reactivity site. Therefore, the design and development of three-dimensional honeycomb nanosilver modified electrode by using the ingenious combination of nano-silver modified electrode and three-dimensional honeycomb porous structure has great potential application value in food, medicine and clinical detection. Because the three-dimensional honeycomb silver electrode is used for quantitative analysis and detection of antibiotics, it has significant advantages such as high selectivity, high sensitivity, short time, simple operation and low cost, and is used for antibiotic detection is the trend, and its application range will be more and more wide.

Acknowledgments

This research was Supported by Hunan Natural Science Foundation (No. 2023JJ50253), Horizontal project of Shaoyang University (No. 2024HX118).

Conflicts of interest

The authors declare that the research was conducted in the absence of any commercial or financial relationships that could be construed as a potential conflict of interest.

References

- [1] S. Ganguli, Z. Zhao, O. Parlak, Y. Hattori, J. Sá, A. Sekretareva, *Angewandte Chemie International Edition*, 62 (2023); <https://doi.org/10.1002/anie.202302394>
- [2] X. Li, Y. Zhou, L. Li, T. Wang, B. Wang, R. Che, Y. Zhai, J. Zhang, W. Li, *Colloids and Surfaces B: Biointerfaces*, 225 (2023); <https://doi.org/10.1016/j.colsurfb.2023.113220>
- [3] Y. Wang, S. Bao, K. Li, N. Zhao, L. Sun, S. Zhang, J. Xin, N. Zhang, *Microchemical Journal*, 208 (2025) 112491; <https://doi.org/10.1016/j.microc.2024.112491>
- [4] H. Jiang, Y. Sun, B. You, *Accounts of Chemical Research*, 56 (2023) 1421-1432; <https://doi.org/10.1021/acs.accounts.3c00059>
- [5] Z. Sun, J. Shen, Y. Pan, Y. Jiang, J. Jiang, *Chemical Engineering Science*, 302 (2025); <https://doi.org/10.1016/j.ces.2024.120845>
- [6] L. Fu, S. Mao, F. Chen, S. Zhao, W. Su, G. Lai, A. Yu, C.T. Lin, *Chemosphere*, 297 (2022) 134127; <https://doi.org/10.1016/j.chemosphere.2022.134127>
- [7] M. Hasanpour, M. Hatami, *Advances in Colloid and Interface Science*, 284 (2020); <https://doi.org/10.1016/j.cis.2020.102247>
- [8] Y.Z. Tingxia Wu, Lingyu Song, Yizhe Chen, Yufu Huang, Junping Tang, Xinzhou Ma, Hanchun Wang, Jun Zhang, Donghai Lin, Guosong Chen, *Anal Methods*, 14(8) (2022) 859-868; <https://doi.org/10.1039/D1AY02051J>
- [9] R. Yu, L. Wang, Q. Xie, S. Yao, *Electroanalysis*, 22 (2010) 2856-2861; <https://doi.org/10.1002/elan.201000296>
- [10] W. Weng, X. Li, W. Nie, H. Liu, S. Liu, J. Huang, Q. Zhou, J. He, J. Su, Z. Dong, D. Wang, *International Journal of Nanomedicine*, 15 (2020) 5027-5042; <https://doi.org/10.2147/IJN.S241859>
- [11] W. Lv, J. Hu, J. Liu, C. Xiong, F. Zhu, *Nanotechnology*, 34 (2023) 165701; <https://doi.org/10.1088/1361-6528/acb4f3>
- [12] G.-C. Chen, W.-T. Huang, P.-C. Lee, C.-B. Lin, *The International Journal of Advanced Manufacturing Technology*, 126 (2023) 797-811; <https://doi.org/10.1007/s00170-023-11177-8>
- [13] J. Yu, F. Chen, Q. Tang, T.T. Gebremariam, J. Wang, X. Gong, X. Wang, *ACS Applied Nano Materials*, 2 (2019) 2679-2688; <https://doi.org/10.1021/acsanm.9b00156>
- [14] Y. Yu, H. Huo, Q. Zhang, Y. Chen, S. Wang, X. Liu, C. Chen, D. Min, *Industrial Crops and Products*, 175 (2022) 114268; <https://doi.org/10.1016/j.indcrop.2021.114268>
- [15] Y. He, Z. Yin, Z. Wang, H. Wang, W. Xiong, B. Song, H. Qin, P. Xu, G. Zeng, *Advances in Colloid and Interface Science*, 304 (2022); <https://doi.org/10.1016/j.cis.2022.102668>
- [16] X. Yang, A. Liu, Y. Zhao, H. Lu, Y. Zhang, W. Wei, Y. Li, S. Liu, *ACS Applied Materials & Interfaces*, 7 (2015) 23731-23740; <https://doi.org/10.1021/acsami.5b07982>
- [17] K. Jin, F. He, Q. Xie, *Journal of Electroanalytical Chemistry*, 849 (2019); <https://doi.org/10.1016/j.jelechem.2019.113375>
- [18] K. Li, YingqiaoZhang, RuochenRen, ShouzhenFeng, XiaojianXue, JingZhang, TongxueZhang, ZixuanHe, ZhangxingDai, LeiWang, Ling, *Colloids and Surfaces, A. Physicochemical and Engineering Aspects*, 602 (2020); <https://doi.org/10.1016/j.colsurfa.2020.125073>

- [19] A.M. Gimenez, R.F. Marques, Matías.Reguart, D.Y. Bargieri, *Frontiers in cellular and infection microbiology*, 11 (2021) 681063; <https://doi.org/10.3389/fcimb.2021.681063>
- [20] H. Jiang, N. Cong, H. Jiang, M. Tian, Z. Xie, H. Fang, J. Han, Z. Ren, Y. Zhu, *International Journal of Hydrogen Energy*, (2023); <https://doi.org/10.1016/j.ijhydene.2023.03.077>
- [21] Y. Li, W.-Z. Jia, Y.-Y. Song, X.-H. Xia, *Chemistry of Materials*, 19 (2007) 5758-5764; <https://doi.org/10.1021/cm071738j>
- [22] W.-Z.J. Ying Li, Yan-Yan Song, Xing-Hua Xia, *Chem. Mater.* 19 (2007) 5758-5764; <https://doi.org/10.1021/cm071738j>
- [23] Y. Li, Y.-Y. Song, C. Yang, X.-H. Xia, *Electrochemistry Communications*, 9 (2007) 981-988; <https://doi.org/10.1016/j.elecom.2006.11.035>
- [24] D. Raj, F. Scaglione, P. Rizzi, *Nanomaterials*, 2023; <https://doi.org/10.3390/nano13010135>
- [25] K. Florey, Cephadrine, in: K. Florey (Ed.) *Analytical Profiles of Drug Substances*, Academic Press, 1976, pp. 21-59; [https://doi.org/10.1016/S0099-5428\(08\)60314-7](https://doi.org/10.1016/S0099-5428(08)60314-7)
- [26] I. Sadeghi, J. Byrne, R. Shakur, R. Langer, *Journal of Controlled Release*, 331 (2021) 503-514; <https://doi.org/10.1016/j.jconrel.2021.01.035>
- [27] R.P. Nagassar, A. Carrington, D.K. Dookeeram, K. Daniel, R.J. Bridgelal-Nagassar, *Antibiotics*, 12 (2023); <https://doi.org/10.3390/antibiotics12071094>
- [28] J. Li, Q. Xue, T. Chen, F. Liu, Q. Wang, C. Chang, X. Lu, T. Zhou, O. Niwa, *Physical Chemistry Chemical Physics*, 23 (2021) 13873-13877; <https://doi.org/10.1039/D1CP01358K>
- [29] A.G. Pisabarro, D.P. Rivera de la Torre, *Preprints*, Preprints, 2020; <https://doi.org/10.20944/preprints202005.0089.v1>
- [30] R. Liu, B. He, H. Jin, Z. Suo, *Analytica Chimica Acta*, 1192 (2022) 339329; <https://doi.org/10.1016/j.aca.2021.339329>
- [31] C. Yuson, K. Kumar, A. Le, A. Ahmadie, T. Banovic, R. Heddle, F. Kette, W. Smith, P. Hissaria, *Internal Medicine Journal*, 49 (2019) 985-993; <https://doi.org/10.1111/imj.14229>
- [32] Y. Sun, J. Zhao, L. Liang, *Microchimica Acta*, 188 (2021); <https://doi.org/10.1007/s00604-020-04671-3>
- [33] C.C. Yingchun Fu, Qingji Xie,, Xiahong Xu, Can Zou, Qingmei Zhou, Liang Tan, Hao Tang, Youyu Zhang, and Shouzhuo Yao, *Anal. Chem* 80 (2008) 5829-5838; <https://doi.org/10.1021/ac800178p>
- [34] E. Bakker, M. Telting-Diaz, *Analytical Chemistry*, 74 (2002) 2781-2800; <https://doi.org/10.1021/ac0202278>
- [35] H.X. You Wang, Jianming Zhang, Guang Li, *Sensors*, 8(4) (2008) 2043-2081; <https://doi.org/10.3390/s8042043>
- [36] X. Li, Z.-Y. Zhang, F. Li, *Chemical Engineering Journal*, 504 (2025) 158101; <https://doi.org/10.1016/j.cej.2024.158101>
- [37] G. Yeom, J. Park, M.-K. Park, J. Hwang, J.-H. Lee, *Sensors and Actuators B: Chemical*, 426 (2025) 137046; <https://doi.org/10.1016/j.snb.2024.137046>
- [38] H.A. Saputra, *Monatshefte für Chemie - Chemical Monthly*, 154 (2023) 1083-1100; <https://doi.org/10.1007/s00706-023-03113-z>

- [39] T. Seesaard, K. Kamjornkittikoon, C. Wongchoosuk, *Science of The Total Environment*, 951 (2024) 175696; <https://doi.org/10.1016/j.scitotenv.2024.175696>
- [40] E. Gorbova, F. Tzorbatzoglou, C. Molochas, D. Chloros, A. Demin, P. Tsiakaras, *Catalysts*, 2022; <https://doi.org/10.3390/catal12010001>
- [41] S. Meenakshi, S. Jancy Sophia, K. Pandian, *Materials Science and Engineering C*, (2018) S0928493117338997; <https://doi.org/10.1016/j.msec.2018.04.064>
- [42] X. Meng, Z. Bi, X. Wang, G. Shang, *The Review of scientific instruments*, 93 (2022) 073707; <https://doi.org/10.1063/5.0096766>
- [43] F. He, Z. Qiao, X. Qin, L. Chao, Y. Tan, Q. Xie, S. Yao, *Sensors and Actuators B: Chemical*, 296 (2019); <https://doi.org/10.1016/j.snb.2019.126679>
- [44] F. Kuralay, A. Erdem, S. Abacı, H. Özyörük, *Colloids and Surfaces B: Biointerfaces*, 105 (2013) 1-6; <https://doi.org/10.1016/j.colsurfb.2012.12.049>
- [45] C. Samdan, *Environmental Science and Pollution Research*, 30 (2023) 99511-99528; <https://doi.org/10.1007/s11356-023-29388-7>
- [46] Q. Yuan, Y. Du, L. Chao, Q. Xie, *Journal of Electroanalytical Chemistry*, 895 (2021) 115416; <https://doi.org/10.1016/j.jelechem.2021.115416>
- [47] F. Huang, S. Qu, S. Zhang, B. Liu, J. Kong, *Talanta*, 72 2 (2007) 457-462; <https://doi.org/10.1016/j.talanta.2006.11.004>
- [48] M.R. Gon?Alves, A. Gomes, J. Conde?O, T.R.C. Fernandes, T. Pardal, C.A.C. Sequeira, J.B. Branco, *Electrochimica Acta*, 102 (2013) 388-392; <https://doi.org/10.1016/j.electacta.2013.04.015>
- [49] Z. Torun, S.H. Boyac, E. Temür, U.U. Tamer, *Biosensors & Bioelectronics*, 37 (2012) 53-60; <https://doi.org/10.1016/j.bios.2012.04.034>
- [50] H.B. Ammar, M.B. Brahim, R. Abdelhédi, Y. Samet, *Materials Science and Engineering: C*, 59 (2016) 604-610; <https://doi.org/10.1016/j.msec.2015.10.025>
- [51] T. Kokulnathan, E.A. Kumar, T.-J. Wang, I.C. Cheng, *Ecotoxicology and Environmental Safety*, 208 (2021); <https://doi.org/10.1016/j.ecoenv.2020.111516>
- [52] J. Mo, S. Wang, J. Zeng, X. Ding, *Journal of Fluorescence*, 33 (2023) 1897-1905; <https://doi.org/10.1007/s10895-023-03184-5>
- [53] F. Pogăcean, C. Varodi, L. Măgeruşan, R.-I. Stefan-van Staden, S. Pruneanu, *Sensors*, 22 (2022); <https://doi.org/10.3390/s22166181>
- [54] M.R. Ali, M.S. Bacchu, M.R. Al-Mamun, M.S. Ahommed, M.A. Saad Aly, M.Z.H. Khan, *RSC Advances*, 11 (2021) 15565-15572; <https://doi.org/10.1039/D1RA02450G>
- [55] H. Zhai, Z. Liang, Z. Chen, H. Wang, Z. Liu, Z. Su, Q. Zhou, *Electrochimica Acta*, 171 (2015) 105-113; <https://doi.org/10.1016/j.electacta.2015.03.140>
- [56] C. Chang, Q. Wang, Q. Xue, F. Liu, L. Hou, S. Pu, *Microchemical Journal*, 173 (2022) 107037; <https://doi.org/10.1016/j.microc.2021.107037>
- [57] F.-F. Gao, Y.-B. Wang, K. Wang, X.-H. Xia, *Journal of Electroanalytical Chemistry*, 781 (2016) 97-102; <https://doi.org/10.1016/j.jelechem.2016.11.001>